EFFECT OF CHARGE PLACEMENT ON FIBRE ORIENTATION, DISTORTION AND FAILURE OF A CARBON FIBRE REINFORCED SHEET MOULDING COMPOUND

Samuel F. Kite[1,2], Ollie Nixon-Pearson[3], Stephen L. Ogin[2], David A. Jesson[2], Ian Hamerton[3], Graham Meeks[1] and Alessandro Sordon[1]

[1]McLaren Automotive Ltd., Woking, Surrey, GU21 4YH, United Kingdom
Email: sam.kite@mclaren.com, graham.meeks@mclaren.com, alessandro.sordon@mclaren.com Web Page: http://cars.mclaren.com
[2]Department of Mechanical Engineering Sciences, University of Surrey, Stag Hill, Guildford, GU2 7XH, United Kingdom
Email: s.kite@surrey.ac.uk, s.ogin@surrey.ac.uk, d.jesson@surrey.ac.uk Web Page: https://www.surrey.ac.uk/minmat
[3]Bristol Composites Institute (ACCIS), Department of Aerospace Engineering, School of Civil, Aerospace, and Mechanical Engineering, Queen's Building, University of Bristol, University Walk, Bristol, BS8 1TR, United Kingdom
Email: on5405@bristol.ac.uk, ian.hamerton@bristol.ac.uk Web Page: http://www.bristol.ac.uk/composites/

Keywords: SMC, discontinuous reinforcement, DIC, warpage, fibre orientation distribution

Abstract

Carbon fibre reinforced sheet moulding compounds are being used more extensively, however their use comes alongside the manufacturing issue of dimensional instability and unpredictable failure locations. These are both features of the fibre orientation distribution which can be affected by the charge location. This paper presents aspects of work examining the effect of the charge placement on the distortion and strain distribution (measured by digital image correlation) of such panels. The warpage of the panel has been compared with an investigation of the fibre orientation distribution by micro-computed tomography. It has been found that the charge location affects both the warpage and strain distribution under load of the moulded panel, with the fibre orientation distribution due to the flow of the charge in the mould being the origin of both effects. To minimise distortion during manufacture, and reduce the negative effects of strain concentrations within the material, the charge shape and placement must be carefully considered during the design process.

1. Introduction

Improved emissions standards, required through such initiatives as the United States' corporate average fuel economy (CAFE) standards, are leading to extensive lightweighting within the automotive industry. The consequence has been an increase in the use of reinforced plastics, but the high cost associated with many manufacturing techniques is preventing more widespread use. To meet the balance between the high strength of traditional carbon fibre reinforced composites, and the rapid manufacture associated with traditional sheet moulding compounds (SMCs), carbon fibre reinforced sheet moulding compounds (C-SMCs) are being used more widely within the automotive industry. However, the use of C-SMCs has generated issues relating to the dimensional stability of components, and difficulties in predicting strengths and fracture locations.

With regard to dimensional stability, it is well known that unfilled polymers, as well as polymer composites, can suffer from warpage. Unfilled polymers will shrink during cure and then undergo mould shrinkage during cooling [1]. Differential shrinkage through the thickness, or in different directions within a component, generates residual stresses [1–3] which can lead to significant warpage if local stiffnesses are low [4]. In filled polymers, warpage caused by these processing paramters generally reduces rapidly as the reinforcement percentage increases [4–6] and it has been shown that the effect on the warpage by the reinforcement is related to differences in the local fibre volume fraction, and the fibre orientation distribution [6,7]. The reinforcement phases tend to have lower coefficients of thermal expansion than the matrix phase (see Table 1, below) and consequently localized areas with higher volume fraction shrink less than those with lower volume fraction, leading to distortion of the panel [8].

Table 1. Coefficients of Thermal Expansion for common matrix and reinforcement materials [9,10].

Material	Coefficient of Thermal Expansion (10^{-6} K^{-1})
Epoxy Resins	60
Polyesters	100-200
Nylon 6,6	90
Polypropylene	110
E-glass	5.4
Kevlar-49	-2.3 - -4.0
Graphite	0.045

The fibre orientation distribution for composites containing fibres with high aspect ratios, will obviously play a large role in distortion/warpage of panels as shrinkage will be different in the transverse and longitudinal directions in areas with highly aligned fibres. Use of a design process that simulates the moulding process and the fibre orientation distribution to optimize the process has been shown to reduce the warpage of components then produced by the process [5,11]. It is worth noting that traditional SMCs do not suffer from such distortions to the same degree due to the use of fillers with low aspect ratios and low profile additives (such as thermoplastics) to reduce shrinkage and improve surface finish.

With regard to the prediction of failure, viewed at a sufficiently large scale C-SMCs may be viewed as homogeneous [12], but their locally heterogeneous nature leads to complexities in predicting both failure strengths and failure locations. The complex failure of this material and its dependence on the fibre orientation distribution is demonstrated by its apparent notch insensitivity [12,13]. Indeed, recent work using micro-computed tomography (µCT) in conjunction with a failure analysis, has emphasized the importance of the difficulty of predicting failure strengths and locations. [14].

The dependence of both the distortion and the failure of components moulded from C-SMC on the fibre orientation distribution therefore requires careful design of the charge for moulding, as this will affect the flow within the mould and therefore the localized fibre orientation distributions. In this work, out-of-plane distortions of a C-SMC panel have been correleated with fibre orientations measured using µCT, and with strain distributions for coupons of the panel under load measured by Digitial Image Correlation (DIC).

2. Materials and Methods

The material used was a tow-based carbon fibre reinforced sheet moulding compound, comprising approximately 12k tows of approximate dimensions 25 mm x 8 mm x 0.2 mm, embedded in an epoxy acrylate matrix; fibre volume fraction of the moulded panel was 0.43. The panel was moulded in a hot press at 140 °C and 10 MPa, with a closing speed of 10 seconds and a cure time of 5 minutes. On removal from the mould, the panel was placed on a flat metal plate to cool. The dimensions of the moulded panel were 200 mm x 200 mm x 2 mm. The charge had a mould coverage of 0.25 (see Figure 1), and was square with dimensions 100 mm x 100 mm, consisting of a stack of four sheets. The charge was placed in the centre of the mould (Figure 1).

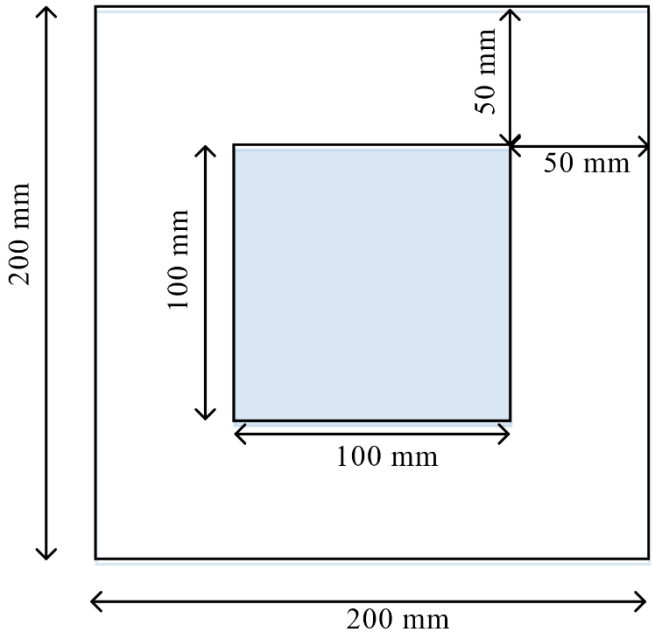

Figure 1. Charge placement (shaded) for moulding of panel

To measure the distortion of the cooled panel, the panel was placed on a flat metal reference plate. A ROMER Absolute Arm, with an integrated laser scanner, was used to scan the panel and Geomagic Qualify software was used to process the point cloud and produce a 3D digital representation of the surface, which compared each of the points to a reference plane. This representation was then used to produce a colour map of the distortion. The panel was cut into four ~50 mm wide tensile-test coupons using a diamond edged Boart saw. The machine used was an Instron 5285 universal testing machine and strain was measured on each face using 3D DIC; *i.e.* two stereo camera systems, operated *via* a control box, with Correlated Solutions software VicSnap and Vic3D used to capture and post-process the images to extract the strains. In order to measure the strain, the coupons were spray painted using a standard off-the-shelf matt white, and then speckled using another off-the-shelf black spray paint; the camera setup is shown in Figure 2. Tensile testing was carried out at a cross head displacement rate of 2 mm s^{-1}. Each coupon was loaded to 2kN for the DIC investigation, unloaded and scanned using µCT, before being tested to failure. To determine the fibre orientation distributions, 4 coupons were scanned in one stack, using a Nikon XTEC XTH 320, with a tungsten target. Due to the size of the tows, scanning at a relatively low resolution was possible since individual fibres did not need to be imaged, reducing the time per scan. The pixel size was 53 µm, with a beam energy of 75 kV, a current of 250 µA, with 3142 projections and 2 frames per projection.

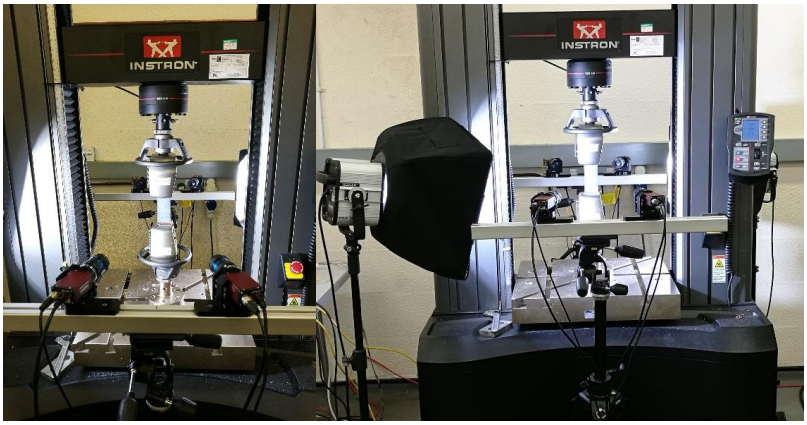

Figure 2. Camera system and lamps set up for DIC on two faces of a specimen.

3. Results and Discussion

3.1 Dimensional Stability

A colour map of the dimensional distortion of the 200 mm x 200 mm panel is shown in Figure 3. The distortion pattern is a saddle shape, with the top right and bottom left corners distorting down (into the page) and the top left and bottom right corners distorting up (out of the page). The top left and bottom right corners had similar levels of distortion (0.70 and 0.51 mm respectively), whilst the top right corner had a much greater distortion than the bottom left (-3.20 mm compared with -0.27 mm). The distortion at the corners to create the saddle shape is due to alignment of the tows as the charge flowed towards the edges of the mould during the compression stage. Of course, the charge has flows in all directions, but it is expected that a greater degree of alignment would take place towards the corners as this was the greatest flow distance. This allows the tows to rotate further to align with the flow, than shorter flow distances. Tow alignment results in the tows resisting shrinkage in the diagonal directions between the corners, leading to the distortion at the corners that can be seen in Figure 3.

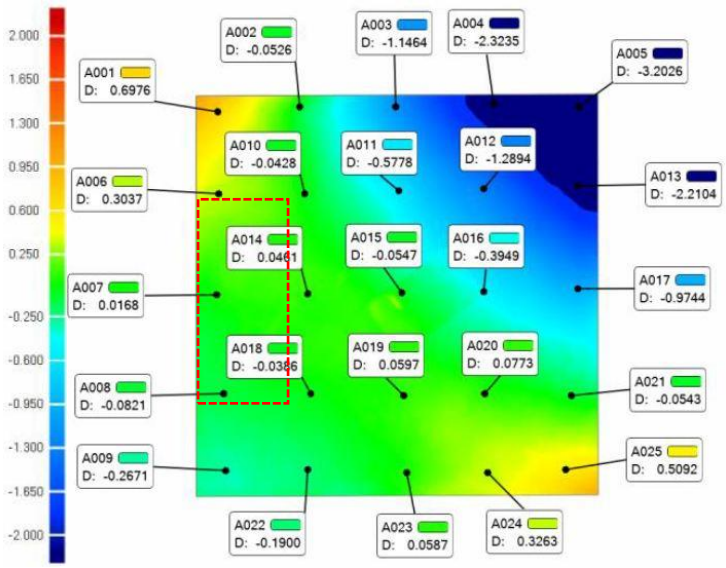

Figure 3. Colour map of the warpage of the panel, including point measurements (mm). The red dashed line indicates the limits of the test coupon investigated by DIC and µCT.

3.2 Strain Distribution Under Load

Figure 3 shows a 50 mm wide section cut from panel, loaded under tension, with the strains measured using DIC. The coupon was loaded to 2 kN and the strain distributions on the front and back face were examined (see Figure 4). The left hand side of the specimen (marked "L") show low ε_{yy} strains, typically a maximum of 600 με (with the y-direction being the loading direction), whilst the right hand edge of the coupon (labelled "R") showing regions of higher strain, up to about 900 με. The high strain feature at the top left corner of the front face is a strain concentration arising as a consequence of gripping the coupon. The low strain areas along "L" suggest a greater alignment of tows in this region in the loading direction. This is expected due to tow realignment as the flow meets the mould edge and is redirected along it. It should also be noted that the front and back faces of the coupon have very different locations of high strain in the DIC images. This is because the tow orientation distribution varies through the thickness, as confirmed by the μCT images.

Images of the same coupon taken using μCT investigation are shown in Figure 5. The images shown, representing slices 53 μm thick, were taken at the surfaces of the coupon i.e. front and back face (Figure 5). It is clear that the tow orientation distribution is quite different which is to be expected because the tow thickness is 0.2 mm within a panel thickness of 2 mm. In the DIC images, both front and back faces have high strain regions along the right hand edge. Comparison of the DIC with the μCT images show that these high strain regions correlate with tows which are oriented transversely to the loading direction. The tows marked A to E in the μCT image (Figure 5) correspond to the high strain regions marked A to E in the DIC image in Figure 4.

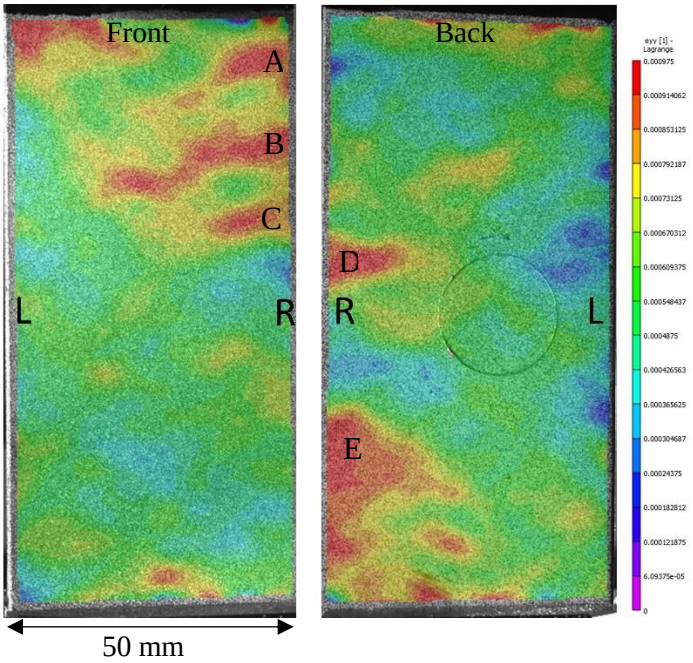

Figure 4. Surface strains on the front and back face, as measured by DIC. The R and L labels indicate the right and left hand sides as viewed from the front face of the specimen.

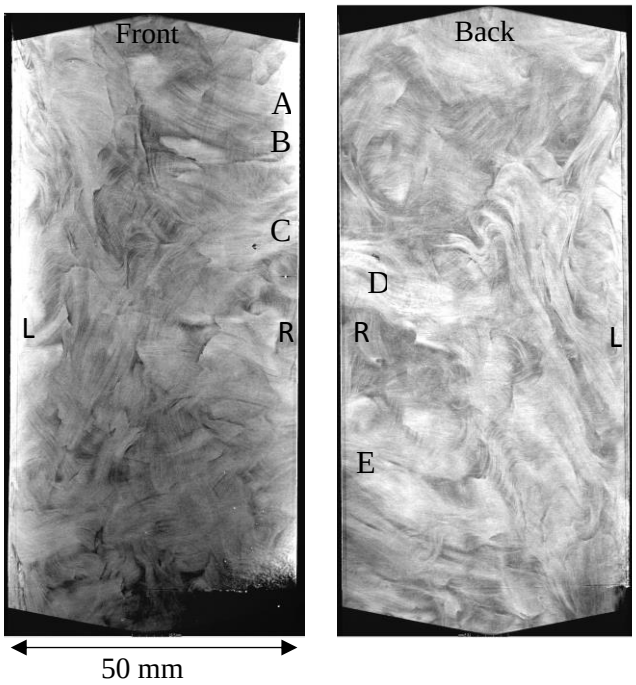

Figure 5. Images of the orientation of carbon fibre tows obtained by μCT for the front and back face of the coupon. The R and L labels indicate the right and left hand sides as viewed from the front face of the specimen.

4. Conclusions

The warpage and strain distribution of a panel manufactured from C-SMC are dependent on the fibre orientation distribution, which is, of course, directly affected by the flow of the charge within the mould. In the work reported here, a 200 mm x 200 mm panel showed an out-of-plane distortion of about 3 mm which is related to the flow within the mold. A combination of μCT and DIC (for a coupon under load) showed that high strain levels in the DIC images corresponded to transversely oriented tows. The results suggest the design of the shape and placement of the charge within the mould cavity must be carefully considered to minimize out-of-plane distortion. The tow orientation distribution varies through the thickness, resulting in different strain distributions on the front and back face, which is related to the difficulty in predicting the strengths and failure locations within components. The effect of varying tow orientation distribution on the failure location will be examined in future work.

Acknowledgments

The authors wish to thank C.P.C Srl for the use of their press in moulding the panels, and McLaren Automotive Ltd., and EPSRC, for funding this research.

References

[1] Zheng R, McCaffrey N, Winch K, Yu H, Kennedy P. Predicting Warpage of Injection Molded Fiber-Reinforced Plastics. J Thermoplast Compos Mater 1996;9:90–106. doi:10.1177/089270579600900107.

[2] Weitsman Y. Residual thermal stresses due to cool-down of epoxy-resin composites. J Appl Mech 1978;46:563–7.

[3] Jensen M, Jakobsen J. Effect of cure cycle on enthalpy relaxation and post shrinkage in neat epoxy and epoxy composites. J Non Cryst Solids 2016;452:109–13.

doi:10.1016/j.jnoncrysol.2016.08.032.

[4] Kikuchi H, Koyama K. Warpage, Anisotropy, and Part Thickness. Polym Eng Sci 1996;36:1326–35. doi:10.1002/pen.10527.

[5] Tseng S-C, Osswald TA. Prediction of Shrinkage and Warpage of Fiber Reinforced Thermoset Composite Parts. J Reinf Plast Compos 1994;13:698–721. doi:10.1177/073168449401300803.

[6] Michii T, Seto M, Yamabe M, Kubota Y, Aoki G, Ohtsuka H. Study on Warpage Behavior and Filler Orientation during Injection Molding. Int Polym Process 2008;23:419–29. doi:10.3139/217.0064.

[7] Kikuchi H, Koyama K. Material anisotropy and warpage of nylon 66 composites. Polym Eng Sci 1994;34:1411–8. doi:10.1002/pen.760341808.

[8] Radford DW. Volume fraction gradient induced warpage in curved composite plates. Compos Eng 1995;5. doi:10.1016/0961-9526(95)00033-J.

[9] Agarwal BD, Broutman LJ. Analysis and performance of fiber composites. Chichester: John Wiley & Sons; 1980.

[10] Hull D, Clyne TW. An introduction to composite materials. Second. Cambridge: Cambridge University Press; 1996.

[11] Yuan Z, Wang Y, Peng X, Wang J, Wei S. An analytical model on through-thickness stresses and warpage of composite laminates due to tool–part interaction. Compos Part B Eng 2016;91:408–13. doi:10.1016/j.compositesb.2016.01.016.

[12] Feraboli P, Peitso E, Cleveland T, Stickler PB, Halpin JC. Notched behavior of prepreg-based discontinuous carbon fiber/epoxy systems. Compos Part A Appl Sci Manuf 2009;40:289–99. doi:10.1016/j.compositesa.2008.12.012.

[13] Qian C, Harper LT, Turner TA, Warrior NA. Notched behaviour of discontinuous carbon fibre composites: Comparison with quasi-isotropic non-crimp fabric. Compos Part A Appl Sci Manuf 2011;42:293–302. doi:10.1016/j.compositesa.2010.12.001.

[14] Denos BR, Kravchenko SG, Pipes RB. Progressive Failure Analysis in Platelet Based Composites Using CT-Measured Local Microstructure. Int SAMPE Tech Conf 2017:1421–35.